PHYSICAL REVIEW B **91**, 235314 (2015)

d-band metal Y_9Co_7 revisited: Evidence for local coexistence of superconductivity and itinerant ferromagnetism

Ł. Bochenek,[1] K. Rogacki,[1] A. Kołodziejczyk,[2] and T. Cichorek[1,*]
[1]*Institute of Low Temperature and Structure Research, Polish Academy of Sciences, Wroclaw, Poland*
[2]*Faculty of Physics and Applied Computer Science, AGH University of Science and Technology, Cracow, Poland*

(Received 27 April 2015; revised manuscript received 29 May 2015; published 15 June 2015)

The heat capacity, magnetic, and electrical transport properties of the binary intermetallic compound Y_9Co_7 are re-investigated through careful low-temperature measurements performed on one and the same high-quality polycrystalline sample. Our results indicate a local coexistence of itinerant ferromagnetism and bulk superconductivity in Y_9Co_7 below $T_{sc} = 2.95$ K, as opposite to a previous conviction that superconductivity occurs in the paramagnetic phase embedded in a basically normal magnetic environment. Since the clean-limit condition is satisfied for a pure sample of Y_9Co_7, the question whether magnetic fluctuations contribute in the formation of Cooper pairs in this sole *d*-band ferromagnetic superconductor remains open.

DOI: 10.1103/PhysRevB.91.235314 PACS number(s): 74.70.Ad, 74.25.Bt, 74.62.Bf

I. INTRODUCTION

A microscopic coexistence of superconductivity (SC) and magnetism is a long-standing but invariably fascinating issue in condensed matter physics. Whereas conventional superconductivity is generally incompatible with magnetism, there is compelling evidence for superconductivity driven by antiferromagnetic fluctuations in various strongly correlated electron systems. A prominent example is the prototypical heavy-fermion compound $CeCu_2Si_2$ [1]. Its low-temperature physical properties, being determined by partially filled Ce-4*f* orbitals, are extremely sensitive to minor variations of the chemical composition. Within the narrow homogeneity range of $CeCu_2Si_2$, either antiferromagnetically ordered (slight Cu deficit) or superconducting (tiny Cu excess) single crystals can be prepared. Samples very close to the nominal 1:2:2 stoichiometry exhibit a ground state where SC and antiferromagnetism compete with each other without microscopic coexistence [2].

Despite enormous effort in new materials design and discovery, coexistence of superconductivity and ferromagnetism is very rare. To date, there are only a few confirmed ferromagnetic (FM) superconductors. $ErRh_4B_4$ is the very first system that shows a long-range FM order far below the superconducting transition [3]. Underlying physics of two spatially separated and mutually exclusive electron subsystems is also realized in $HoMo_6S_8$ [4] and $ErNi_2B_2C$ [5]. Whereas all these materials are very interesting on their own, an exciting possibility concerns a situation when the conduction electrons are both ferromagnetically ordered and superconducting. An evidence for an interplay between SC and ferromagnetism in the same electron system was found in UGe_2 [6] and the related U-5*f* materials [7,8]. Pressure-induced superconductivity of UGe_2 occurs on the border of itinerant ferromagnetism, while Cooper pairs in URhGe [7] and UCoGe [8] are formed deep in the FM state at ambient conditions. Remarkable that such a cooperative coexistence gives rise to an unconventional paring mechanism. However, for the latest member of this family, a possible contribution of partially filled Co-3*d* orbitals to a FM ground state with a very small ordered magnetic moment $\mu_{\text{ord}} \approx 0.05\ \mu_B$/f.u. remains to be unambiguously excluded, since a strong influence of sample preparation technology and treatment has been observed [9,10].

About the same time as the discovery of superconductivity in the heavy-fermion compound $CeCu_2Si_2$, weak itinerant ferromagnetism with a Curie temperature $T_C \approx 4.5$ K and superconductivity below a critical temperature $T_{sc} \approx 2.5$ K were observed in the *d*-electron system of Y_9Co_7 (at that time considered as Y_4Co_3) [11]. However, a complexity of the binary chemical Y-Co phase diagram and ambiguities concerning an origin of magnetic electrons and superconducting carriers have limited interest in this exotic material [12]. While a zero resistivity below 2 K was observed in a number of polycrystalline Y_9Co_7 samples, traces of superconducting anomaly were detected only in a few specific-heat experiments. In contrast, magnetic properties appear to be weakly sample dependent, but a very small value of $\mu_{\text{ord}} \approx 0.08\ \mu_B$/f.u. has hampered progress in understanding. Nevertheless, the Curie temperature T_C of about 4.5 K is rather well established from, e.g., the conventional Arrott-plot analysis of the isothermal magnetization [13]. All those observations lead to a conclusion that superconductivity occurs in the paramagnetic phase embedded in a basically normal magnetic environment. For a review of the experimental data we address the reader to [14,15].

Y_9Co_7 crystallizes in the hexagonal ($P6_3/m$) Ho_4Co_{3+x} structure with the lattice parameters $a = 11.528$ Å and $c = 12.153$ Å [16–18]. The unit cell is rather complex with two inequivalent positions for the Y atoms and three different positions for the Co atoms. The Co atoms at the 2*b* site are octahedrally coordinated by the Y(1) atoms and form chains along the *c* axis, whose period is strongly altered by a substantial deficiency in the Co(2*b*) occupancy. The Co atoms at the 2*d* and 2*h* sites are prismatically coordinated by the Y(2) atoms. Recently performed first-principles calculations have confirmed previous suggestions that weak ferromagnetism arises only from the Co(2*b*) atoms, while remaining Co and Y atoms act as a diamagnetic environment [15].

Here we present results of the extensive investigations of Y_9Co_7 via electrical resistivity, dc magnetization, ac susceptibility, and specific heat measurements in zero and

---

[*] Corresponding author: t.cichorek@int.pan.wroc.pl

applied magnetic fields down to the milli-Kelvin temperature range. All the data were obtained for the same sample with the highest critical temperature $T_{sc} = 2.95(5)$ K ever reported. Our results indicate that superconductivity is a bulk property of Y_9Co_7 and, more importantly, SC coexists with FM order in a sample satisfying the clean-limit condition.

II. EXPERIMENT

Y_9Co_7 was prepared by arc melting of high-purity yttrium from the Ames Research Laboratory together with 5N Johnson-Matthey cobalt in a high-purity argon atmosphere. The as-cast ingot, placed in an evacuated quartz ampoule, was annealed at 850 K for two weeks and subsequently at 750 K for six weeks. After this heat treatment, powder x-ray diffraction measurements indicated a minor amount (<2 vol. %) of impurity phases. The polycrystalline specimen with dimensions 2.64 mm $\times$ 0.41 mm $\times$ 0.36 mm and a total mass of 2.12 mg was cut off from the interior of the ingot by a wire saw, and finally irregular surfaces were polished.

For the reasons mentioned above, it is of crucial importance to measure physical properties of Y_9Co_7 on one and the same sample: the magnetization M, both as a function of temperature and magnetic field, was measured using a Quantum Design superconducting quantum interference device magnetometer (MPMS). The temperature-dependent ac susceptibility $\chi_{ac}(T)$ was determined in the drive field $B_{ac} = 100\,\mu$T utilizing a Quantum Design physical property measurement system (PPMS). Supplementary $\chi_{ac}(T)$ measurements down to 0.15 K were performed with $B_{ac} = 20\,\mu$T utilizing a ^{3}He - ^{4}He dilution refrigerator. The specific heat $C(T)$ was determined with the aid of the thermal-relaxation method utilizing a commercial ^{3}He microcalorimeter (PPMS). After completing magnetic and specific-heat experiments [19], the electrical resistivity $\rho(T)$ was monitored by a standard four-point ac technique in zero and applied magnetic fields up to 14 T at temperatures as low as 0.07 K. Zero-field $\rho(T)$ measurements above 20 K were performed in a ^{4}He cryostat. Electrical contacts were made by spot welding 25 μm gold wires to the sample.

III. RESULTS AND DISCUSSION

In Fig. 1 we present the magnetic properties of Y_9Co_7. The main panel shows the temperature dependence of the magnetization measured in $B = 3$ mT after zero field cooling. Below 8 K, $M(T)$ increases by more than one order of magnitude and thus signals a ferromagnetic transition. At the temperature where superconductivity emerges ($\simeq 3$ K), a FM order is not yet completed and hence a crude estimation of an ordered moment yields $\mu_{ord} \approx 0.06(1)\,\mu_B$/f.u. Ferromagnetism is further corroborated by a hysteresis loop in $M(B)$ at 2 K (see the lower inset of Fig. 1). In the superconducting state, a diamagnetic signal is superimposed on a FM signal giving rise to an unusual $M(B)$ dependence of the first magnetization curve (open symbols). Apparently, a virgin curve beyond the hysteresis loop reflects anomalous vortex dynamics in the FM superconductor Y_9Co_7, but it is beyond the scope of this paper. Finally, the FM transition shows up as a broad anomaly in the real part of the ac susceptibility χ'_{ac} around the liquid helium temperature. Below 3 K, Y_9Co_7 becomes superconducting as seen by a large diamagnetic signal in χ'_{ac}. We also note that the in-phase component saturates upon cooling below 1 K, thus suggesting the complete superconducting transition in our sample.

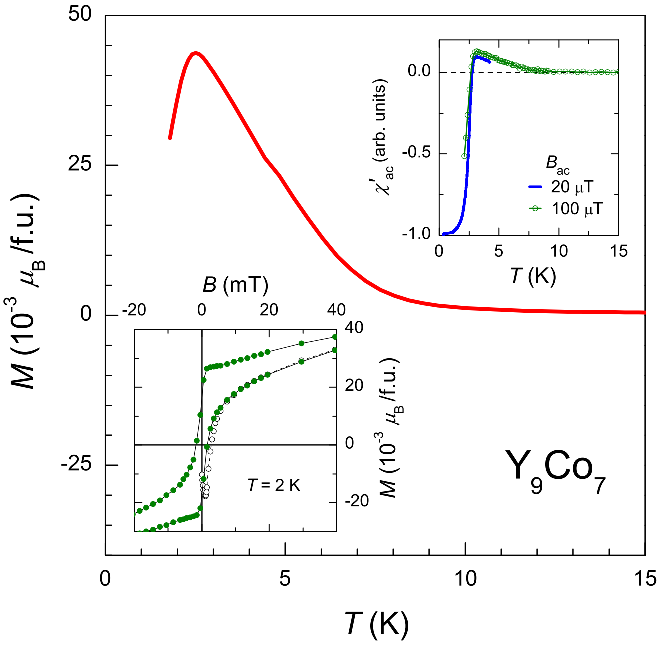

FIG. 1. (Color online) Low-temperature magnetization of Y_9Co_7 measured in $B = 3$ mT (obtained after completing the resistivity measurements). Below $T \sim 8$ K, an increase of $M(T)$ indicates a ferromagnetic order. For $T < 2.5$ K, a rapid drop due to superconductivity emerges. Bottom inset: FM hysteresis loop in $M(B)$ at 2 K with superimposed diamagnetic signal due to superconductivity. Top inset: ac susceptibility vs temperature measured in $B_{ac} = 20$ and 100 μT down to $T = 0.15$ and 1.8 K, respectively.

The low-temperature dependence of the electrical resistivity $\rho(T)$ of Y_9Co_7 is illustrated in Fig. 2. Below 8 K, the resistivity quasilinearly decreases down to the emergence of superconductivity. There is no obvious anomaly in $\rho(T)$ due to ferromagnetism. Note that an anomaly around T_C was detected in none of the earlier studies. A residual resistivity $\rho_0 = 6.9(4)\ \mu\Omega$ cm, estimated from a zero-field $T^{3/2}$ dependence (see below), is very close to 6.6 $\mu\Omega$ cm formerly reported for the high-purity sample [20]. As shown in the inset of Fig. 2, an overall $\rho(T)$ behavior with a room temperature value of $\rho_{300\,K} = 178(11)\ \mu\Omega$ cm is similar to those reported in the literature. As a result, we obtained a residual resistivity ratio RRR $= \rho_{300\,K}/\rho_0 \simeq 26$, the large value of which reflects the high quality of our sample. This is further evident in such superconducting parameters as the highest value of $T_{sc} = 2.95(5)$ K reported to date and a resistive onset temperature of 3.75(5) K. Also, a resistive transition $\Delta T_{sc}/T_{sc} \approx 0.15(3)$ is sharper compared to the previous reports for Y_9Co_7 [11,21]. Nonzero value of the resistivity, observed down to $T = 0.07$ K, is an artifact due to a spot-welding technique necessarily used to produce the low-resistance electrical contacts. This adverse observation reflects complex metallurgical properties of a binary Y-Co phase diagram. Most likely, spot welding locally produced a

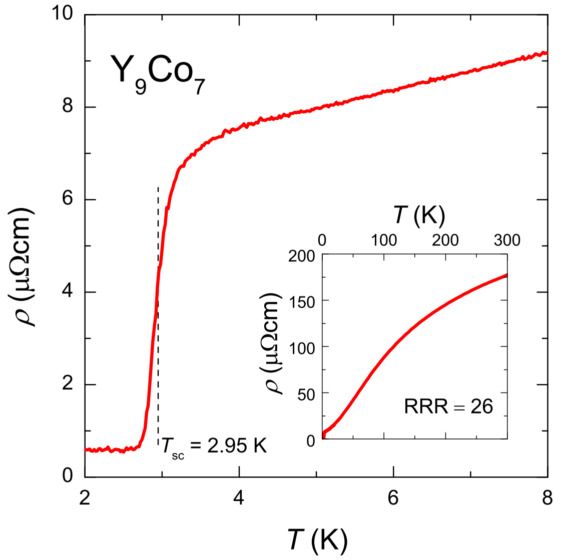

FIG. 2. (Color online) Electrical resistivity of a polycrystalline Y_9Co_7 sample in the vicinity of the superconducting transition. The superconducting critical temperature $T_{sc} = 2.95$ K, marked by the dashed line, was determined from a midpoint of the resistivity drop adopting the 10%–90% criterion. Inset: Electrical resistivity in the whole temperature range.

nonmagnetic and nonsuperconducting impurity phase such as, e.g., Y_8Co_5 [22,23].

According to the self-consistent renormalization theory [24], the resistivity of an itinerant ferromagnet should follow a T^n power law, with $n = 2$ and $5/3$ in the temperature range below and above T_C, respectively. Such a resistivity dependence is seen in various itinerant ferromagnetic metals. In particular, this holds true for the superconducting ferromagnet UCoGe with the Curie temperature of 3 K. For this material, it is believed that the same $5f$-electron system is responsible for a coexistence of weak ferromagnetism and unconventional SC below $T_{sc} \approx 0.6$ K. Most likely, a very small ordered moment $\mu_{ord} \approx 0.05\,\mu_B$ is on the U atoms forming the zigzag structure [25], though an impact of partially filled Co-$3d$ orbitals is not yet satisfactory explained [26]. Quite different behavior of the paramagnetic-state $\rho(T)$ data is seen for the weak $4f$-derived metallic ferromagnet $YbNi_4P_2$ with $T_C = 0.15$ K. In the temperature window $0.15 \leqslant T \leqslant 1$ K, the resistivity of this heavy-fermion compound is quasi-T linear [27]. Such an unusual behavior suggests strong FM quantum critical fluctuations. In the presence of a Kondo screening, the magnetic Yb^{3+} ions form chains with the ordered moment of about $0.05\,\mu_B$.

We now turn to an influence of a magnetic field on the normal-state electrical resistivity of Y_9Co_7. This study, missing in previous experiments, provides important information on magnetic fluctuations in this d-band metal. Figure 3(a) presents the resistivity data of Y_9Co_7 measured below 20 K in varying magnetic fields aligned with the electrical current [28]. In zero field, $\rho(T) = \rho_0 + cT^{3/2}$ with $c = 101(1)\ \mu\Omega\,\mathrm{cm}\,\mathrm{K}^{-3/2}$ is observed down to the onset of superconductivity [cf. the inset of Fig. 3(a)]. The temperature exponent $n = 3/2$ is slightly lower than $5/3$ typically caused by electron scattering off critical ferromagnetic spin fluctuations [24]. The lower $n = 3/2$ value apparently reflects a low dimensionality of the ferromagnetic Co($2b$) substructure. A slope of the $T^{3/2}$ dependence only weakly depends on an applied magnetic field and approaches a value of $106(1)\ \mu\Omega\,\mathrm{cm}\,\mathrm{K}^{-3/2}$ at $B = 1$ T. (We note that in this field a small fraction of our Y_9Co_7 sample still displays surface superconductivity below about 1 K.) At larger fields, the

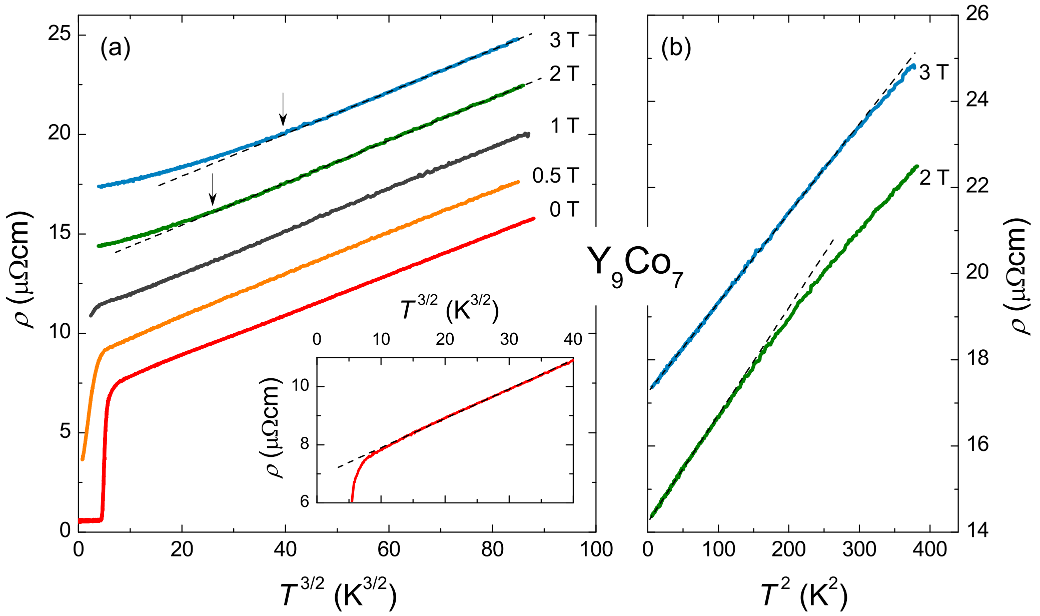

FIG. 3. (Color online) (a) Low-temperature resistivity of Y_9Co_7 on a $T^{3/2}$ scale in varying magnetic fields aligned with the electrical current. For clarity, the different $\rho(T)$ curves in finite fields were shifted upwards subsequently by $2\ \mu\Omega\,\mathrm{cm}$. The dashed lines emphasize a $T^{3/2}$ power law observed down to 8.8 and 11.7 K at $B = 2$ and 3 T, respectively. Inset: Zero-field $\rho(T)$ vs $T^{3/2}$ below 12 K. (b) Resistivity versus T^2 in fields of 2 and 3 T.

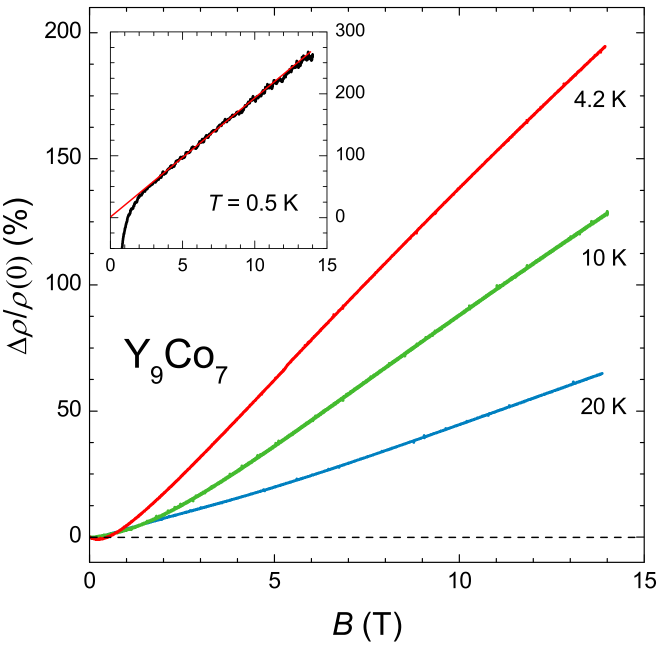

FIG. 4. (Color online) Longitudinal magnetoresistance $\Delta\rho/\rho(0)$ for polycrystalline Y_9Co_7 as a function of magnetic field B up to 14 T at $T = 4.2$, 10, and 20 K. Inset: Magnetoresistance obtained at $T = 0.5$ K. Here $\rho(0)$ corresponds to a zero-field intercept of the linear MR.

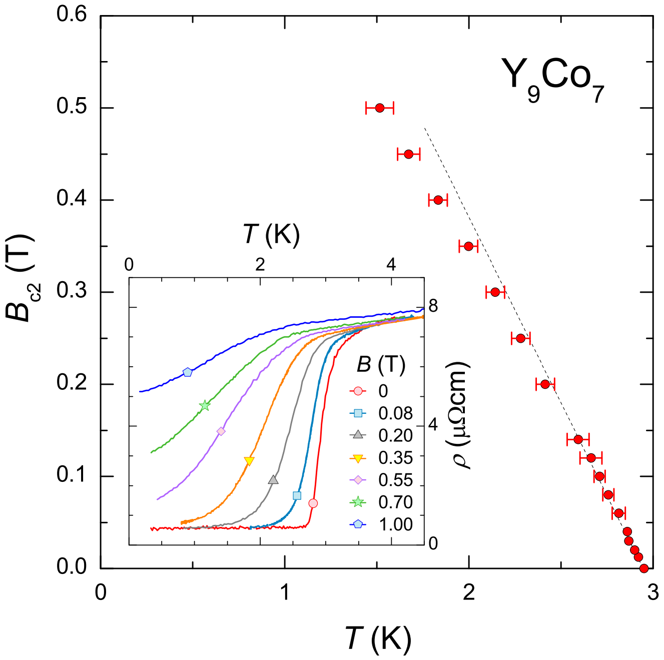

FIG. 5. (Color online) Temperature dependent upper critical field $B_{c2}(T)$ of Y_9Co_7 as obtained from the resistivity measurements. The upper critical field B_{c2} was determined by the midpoints of the resistivity drop adopting the 10%–90% criterion in fixed magnetic fields. The dashed line represents the initial slope $(-dB_{c2}/dT)_{T_{sc}} = 0.37$ T/K. Inset: Typical $\rho(T)$ dependencies used to determine $B_{c2}(T)$.

coefficient c remains unchanged but the $T^{3/2}$ behavior has been narrowed down, as marked by arrows. At lower temperatures, least-square fits reveal a proper $\rho(T) \propto aT^2$ behavior with the magnetic-field-dependent coefficient $a = 0.024(1)$ and $0.021(1)$ $\mu\Omega\,\mathrm{cm\,K^{-2}}$ for $B = 2$ and 3 T, respectively [cf. Fig. 3(b)]. Certainly the unusual low-T dependence of the electrical resistivity and its anomalous response to an external field give evidence of magnetism in Y_9Co_7 that we relate to FM fluctuations within the Co(2b) chains.

The magnetoresistance (MR) data for polycrystalline Y_9Co_7 are shown in Fig. 4 as $\Delta\rho/\rho(0)$ vs B, where $\Delta\rho = \rho(B) - \rho(0)$. The measurements were performed in the temperature window $0.5 \leqslant T \leqslant 20$ K, where substantial spin fluctuations were observed in the $\rho(T)$ dependencies at $B =$ const. An interesting feature is a linear magnetoresistance in classically strong magnetic fields, i.e., when a gyroradius of conduction electrons becomes smaller than their mean free path. At 0.5 K, the MR as large as 260% was found in $B = 14$ T (cf. the inset in Fig. 4). With increasing temperature up to 20 K, a slope of $\Delta\rho/\rho(0)$ decreases by a factor of nearly 4. Such a positive, nonsaturating, and dominantly linear-in-B magnetoresistance is frequently observed in samples being composed of a chemically homogeneous mixture of irregular crystallites of a metal with open Fermi surface [29]. Although a Fermi surface of the d-band metal Y_9Co_7 has not yet been determined, one can safely assume its open character owing to a number of various open orbits of the Fermi surfaces of elemental 3d yttrium and 4d cobalt [30,31]. As a result of these points, a linear response of the resistivity to an applied magnetic field indicates a good chemical homogeneity of the sample investigated.

Figure 5 displays the temperature dependent upper critical field $B_{c2}(T)$ of Y_9Co_7 as determined from the electrical resistivity measured at $B < 0.6$ T. Details of the $\rho(T,B)$ dependence in the vicinity of the superconducting transition is shown in the inset of Fig. 5. The slope of the upper critical field $(-dB_{c2}/dT)_{T_{sc}} = 0.37(3)$ T/K is very close to the value recently deduced from the magnetization data for another Y_9Co_7 specimen from the same ingot [32]. Thus, the resistivity results obtained in small magnetic fields lead to essentially the same estimation for the coherence length $\xi \approx 240$ Å and the electron mean free path $l \approx 2220$ Å. Consequently, we came to the conclusion that with increasing chemical purity and reduction of structural disorder the d-band ferromagnetic superconductor Y_9Co_7 can be tuned to the clean limit. (Some other superconducting parameters, evaluated via the isotropic Ginzburg-Landau-Abrikosov-Gor'kov theory and the Werthamer-Helfand-Hohenberg model, are listed in Ref. [32].)

The specific heat $C(T)$ of Y_9Co_7 was investigated on the specimen that satisfies the $l \gg \xi$ condition. Although its total heat capacity is very small [e.g., 0.94(1) $\mu\mathrm{J\,K^{-1}}$ at the liquid helium temperature], we were able to precisely determine the low-temperature $C(T)$ dependence of Y_9Co_7 utilizing a modern thermal-relaxation microcalorimeter. Figure 6(a) shows our specific-heat data as C/T vs T^2, obtained between 0.4 and 12.5 K. Assuming that the specific heat above 7 K follows a simple $\gamma T + \beta T^3$ dependence (where γ is the Sommerfeld coefficient and β is proportional to the Debye temperature Θ_D), a least-squares fit reveals $\gamma = 62(1)$ $\mathrm{mJ\,K^{-2}\,mol^{-1}}$ and $\Theta_D = 228(2)$ K $[\beta = 2.623(5)$ $\mathrm{mJ\,K^{-4}\,mol^{-1}}]$. While our

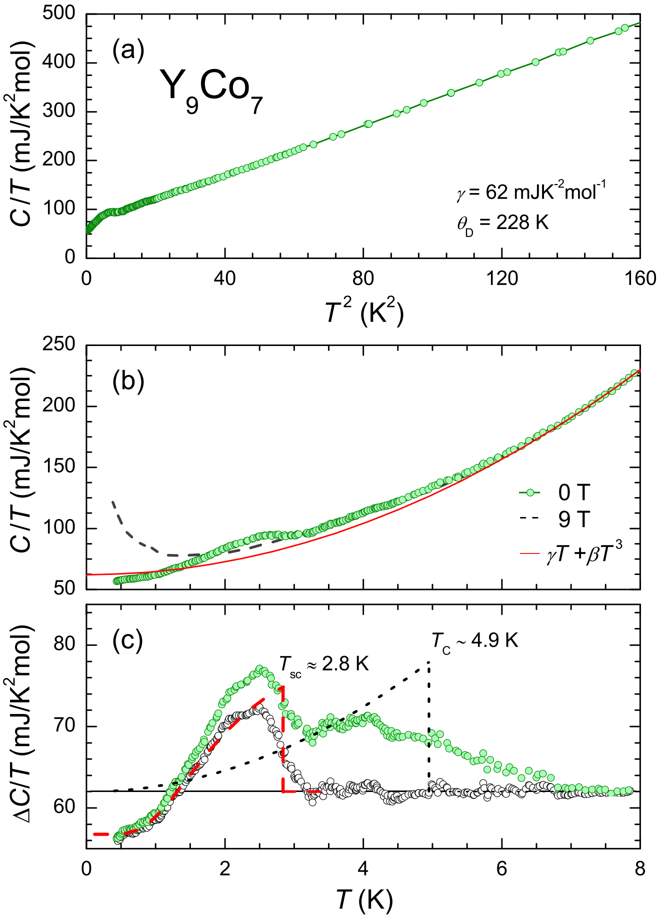

FIG. 6. (Color online) Solid evidence for the bulk interplay between ferromagnetism and superconductivity in Y_9Co_7: (a) Specific heat divided by temperature C/T versus T^2 in zero magnetic field. (b) Comparison of the zero field and $B = 9$ T specific heat shown as C/T versus T. The solid line gives a usual $C = \gamma T + \beta T^3$ dependence. (c) Electronic and magnetic contributions to specific heat of Y_9Co_7, as $\Delta C/T$ versus T. The gray points indicate the electronic specific heat obtained after subtraction of the FM contribution whose temperature dependence below 3 K was approximated by the idealized FM (dashed-dotted line) transition with a step size at 4.9 K. The dashed line gives an idealized superconducting transition using an equal entropy construction with a residual γ_0 value of 56 mJ K^{-2} mol^{-1}.

estimation of the lattice contribution is in satisfactory agreement with the previous results [21,33,34], there are some differences in a linear term in the electronic specific heat. A variation of γ by a factor of 2, i.e., between 24 and 54 mJ K^{-2} mol^{-1} [21,33,34], should be ascribed to difficulties inherent to old experimental techniques and ambiguities concerning the true chemical composition (Y_4Co_3 vs Y_9Co_7).

To gain more insight into the specific-heat data in the vicinity of the ferromagnetic and superconducting transitions, the C/T results are shown in Fig. 6(b) on a linear T scale. At about 7 K, the specific heat starts to deviate from the $\gamma T + \beta T^3$ dependence (marked by solid line) due to a presence of the magnetic contribution. The FM transition shows up as a small and broad feature down to about 3.5 K. Upon further cooling, a clear superconducting anomaly emerges. At the milli-Kelvin temperatures, the specific heat is smaller than values expected for nonsuperconducting and paramagnetic Y_9Co_7. We emphasize that such a clear thermodynamic signature of superconductivity was observed in none of earlier experiments on Y_9Co_7 [21,33].

Additionally displayed in Fig. 6(b), as a dashed line, are the 9 T data that essentially follow the zero-field results above 3.5 K. This finding suggests a weak influence of external magnetic fields $B \leqslant 9$ T on ferromagnetism in Y_9Co_7. Such like observation, though made at a smaller field of 5 T, was previously reported for the sample with a hardly visible anomaly at T_{sc} [34]. We also note that upon cooling below about 1.2 K in $B = 9$ T, an upturn in C/T due to the nuclear Schottky contribution C_n develops whose origin is mainly caused by Co nuclei (nuclear spin $I = 7/2$ for ^{59}Co with the natural abundance of 100%). While more experimental input is needed to separate the nuclear term from the total heat capacity, we anticipate a substantial contribution of $C_n(T)$ also in the absence of an external field. This is because of both the strong intrasite hyperfine coupling between the nucleus and 3*d* electrons on the same Co(2*b*) ion and the nuclear electric quadrupole moment of the ^{59}Co isotope, the only component in Y_9Co_7 that possesses a nuclear spin larger than 1/2.

A semiqualitative analysis of the low-*T* specific heat for Y_9Co_7 is shown in Fig. 6(c). Here ΔC denotes $C - C_{latt}$, where $C_{latt} = \beta T^3$. In this plot, both anomalies at $T_C \sim 4.9$ K and $T_{sc} \simeq 2.8$ K are clearly visible, thought the FM transition is broad. The relative change $(\Delta C/T_C)/(C/T_C)$ assuming an ideal transition [see dashed-dotted line in Fig. 6(c)] is only 26% and the magnetic entropy associated with the transition is small (0.45% of *R*ln2). We emphasize that quite similar estimations (25% and 0.3%, respectively) were made at an early period of research on UCoGe, the system where the interplay between ferromagnetism and SC occurs at ambient conditions ($T_C = 3$ K and $T_{sc} \simeq 0.6$ K) [8,9].

A rough estimate for the step size of the superconducting transition in the specific heat (dashed line) can be obtained after subtraction of the idealized ferromagnetic contribution. Using an equal entropy construction with $T_{sc} \simeq 2.8$ K we obtained $\Delta C/\gamma T_{sc} \sim 0.2$ that is 7 times smaller than the BCS value (=1.426). Note that considerably smaller $\Delta C/\gamma T_{sc}$ than a conventional BCS prediction was also reported for high-quality single-crystalline samples of UGe_2, URhGe, and UCoGe [25]. It is believed that these systems are in the superconducting mixed state even at zero applied field. This is because the ordered moment gives rise to an internal field considerably larger than the lower critical field. As a consequence, a small superconducting anomaly in zero applied field appears to be a quite natural property of FM superconductors. For Y_9Co_7 with the ordered moment as small as in UCoGe, an impact of the internal field might be even stronger because of its relatively low upper critical field.

Another consequence of the self-induced vortex state in U-based ferromagnetic superconductors is a large value of the residual electronic specific heat coefficient $\gamma_0 = C(T)/T$ measured at the lowest temperatures. For the best quality samples, a γ_0/γ ratio varies from 0.15 to 0.7 for UCoGe (RRR = 165) and UGe_2 (RRR = 600), respectively [25]. For our Y_9Co_7 specimen, we found $\gamma_0/\gamma \simeq 0.9$ at 0.4 K [cf. Fig. 6(c)] which could be somewhat underestimated,

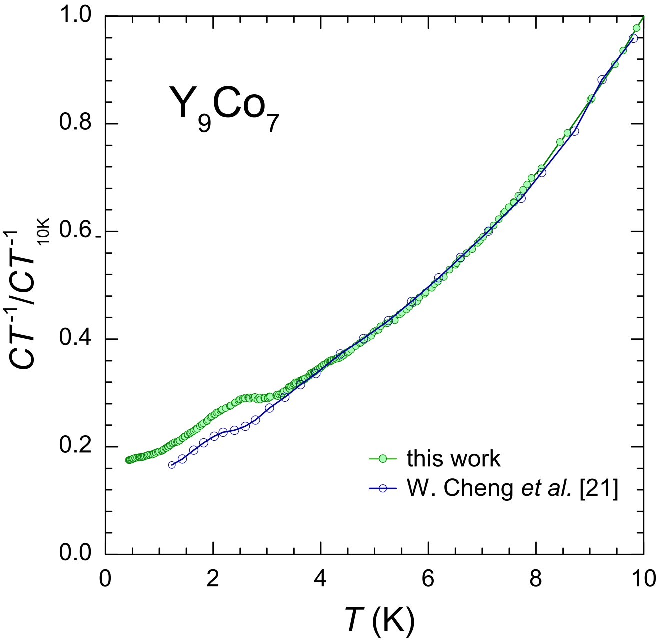

FIG. 7. (Color online) Comparison of the specific heat data for various samples of Y_9Co_7. The results, shown as C/T versus T, were normalized to the corresponding value at 10 K. The superconducting critical temperature, determined from the resistivity measurements, amounts to $T_{sc} \approx 2.5$ K (open points [21]) and $T_{sc} = 2.95$ K (solid points, this work).

because a $C_n(T)$ contribution likely accounts for a large fraction of the specific heat at milli-Kelvin temperatures, as discussed above. Lastly, we emphasize that the smaller heat capacity in the superconducting state than in the normal state has not been observed for any other samples so far. In other words, we have shown that the entropy is substantially lower in the superconducting state when the Y_9Co_7 system is tuned to the clean limit. This observation additionally highlights SC as a bulk property of this *d*-band metal.

Our studies indicate that a local coexistence of superconductivity and itinerant ferromagnetism occurs in Y_9Co_7. This is especially evident in the specific-heat results. Indeed, for the sample that satisfies the clean-limit condition we found several characteristics of a superconducting ferromagnet exemplified in UCoGe. This inference is further corroborated by an examination of the literature. In Fig. 7 we compare our C/T data with the results by Cheng *et al.* for the Y_4Co_3 (nominal composition) sample whose $T_{sc} \approx 2.5$ K was evidenced by the resistivity measurements [21]. These are the most complete specific heat data among a few others reported for Y_9Co_7/Y_4Co_3 to date. Having regard to different notations, both sets of the C/T results were normalized to the corresponding value at 10 K. Down to about 3.5 K, there are negligible differences between our and literature data. This holds particularly true for the anomaly due to weak itinerant ferromagnetism. In striking contrast to similar properties of the normal state are the C/T results below 3.5 K. In this temperature range, our data distinctly differ from these by Cheng *et al.* [21] which display a hardly visible anomaly due to superconductivity. Taken together, the comparison of C/T vs T shown in Fig. 7 implies that the superconducting fraction grows up with increasing sample quality. By essentially unaltered FM contribution, this observation presents evidence for a local coexistence of superconductivity and itinerant ferromagnetism in Y_9Co_7.

Unlike in the uranium-based superconducting ferromagnets, the different electron subsystems are responsible for SC and ferromagnetism in Y_9Co_7. However, as opposite to local, full-moment FM superconductor $ErRh_4B_4$ [3], $HoMo_6S_8$ [4], and $ErNi_2B_2C$ [5], ferromagnetism in Y_9Co_7 is mediated by the extended orbitals that contribute to the density of states at the Fermi level. Thus, this *d*-band metal provides an unique opportunity to study a coexistence of SC and ferromagnetism of mutually interacting electron subsystems. Early stage finding that external pressure suppresses magnetism and enhances superconductivity [35] may suggest a key experiment to disclose peculiarities of Y_9Co_7. An exciting possibility concerns enhancement of superconductivity near a ferromagnetic quantum critical (end) point in the 3*d*-4*d* electron system. Such an observation would indicate that the interplay between weak itinerant ferromagnetism and superconductivity is cooperative rather than competing. It remains to be solved to what extend physical properties of Y_9Co_7 depend on minor variations of the chemical composition within a likely narrow homogeneity range or/and are ordinary influenced by off-stoichiometric Y/Co contaminations. Clearly studies on single-crystalline samples of Y_9Co_7 are of prime importance, especially owing to the quasi-one-dimensional character of the ferromagnetic order.

IV. CONCLUSIONS

Transport, magnetic, and thermodynamic properties of intermetallic compound Y_9Co_7 have been re-investigated employing modern experimental techniques. All experiments were performed on one and the same polycrystalline sample whose high quality is evidenced by, e.g., a small residual resistivity of 6.9 $\mu\Omega$ cm and a correspondingly large residual resistivity ratio of 26.

Magnetization measurements underline itinerant ferromagnetism with a small ordered moment of $\approx 0.06\ \mu_B$/f.u. as an intrinsic property of Y_9Co_7. For this *d*-band metal, superconductivity at $T_{sc} = 2.95$ K is suggested by both a large diamagnetic signal in the ac susceptibility and a sharp drop of the electrical resistivity. The specific heat provides solid evidence for the bulk interplay between superconductivity and weak itinerant ferromagnetism in the Y_9Co_7 sample that satisfies the clean-limit condition.

The results on Y_9Co_7 reported here together with an examination of the literature data imply the coexistence superconductivity with weak itinerant ferromagnetism on a microscopic scale, opposite to previous beliefs that a small fraction of the superconducting state occurs in the paramagnetic phase embedded in a predominantly normal magnetic medium. Since Y_9Co_7 displays both SC and FM order at ambient conditions, this *d*-band metal offers a rare opportunity to study the condensation of Cooper pairs in the presence of a molecular field.

[1] F. Steglich, J. Aarts, C. D. Bredl, W. Lieke, D. Meschede, W. Franz, and H. Schäfer, Phys. Rev. Lett. **43**, 1892 (1979).

[2] F. Steglich, P. Gegenwart, C. Geibel, R. Helfrich, P. Hellmann, M. Lang, A. Link, R. Modler, G. Sparn, N. Büttgen, and A. Loidl, Physica B **223-224**, 1 (1996).

[3] W. A. Fertig, D. C. Johnston, L. E. DeLong, R. W. McCallum, M. B. Maple, and B. T. Matthias, Phys. Rev. Lett. **38**, 987 (1977).

[4] M. Ishikawa and O. Fischer, Solid State Commun. **23**, 37 (1977).

[5] P. C. Canfield, S. L. Bud'ko, and B. K. Cho, Physica C **262**, 249 (1996).

[6] S. S. Saxena, P. Agarwal, K. Ahilan, F. M. Grosche, R. K. W. Haselwimmer, M. J. Steiner, E. Pugh, I. R. Walker, S. R. Julian, P. Monthoux, G. G. Lonzarich, A. Huxley, I. Sheikin, D. Braithwaite, and J. Flouquet, Nature (London) **406**, 587 (2000).

[7] D. Aoki, A. Huxley, E. Ressouche, D. Braithwaite, J. Flouquet, J. P. Brison, E. Lhotel, and C. Paulsen, Nature (London) **413**, 613 (2001).

[8] N. T. Huy, A. Gasparini, D. E. de Nijs, Y. Huang, J. C. P. Klaasse, T. Gortenmulder, A. de Visser, A. Hamann, T. Göerlach, and H. von Löehneysen, Phys. Rev. Lett. **99**, 067006 (2007).

[9] A. Gasparini, Y. K. Huang, N. T. Huy, J. C. P. Klaasse, T. Naka, E. Slooten, and A. de Visser, J. Low Temp. Phys. **161**, 134 (2010).

[10] J. Pospíšil, K. Prokeš, M. Reehuis, M. Tovar, J. P. Vejpravová, J. Prokleška, and V. Sechovský, J. Phys. Soc. Jpn. **80**, 084709 (2011).

[11] A. Kołodziejczyk, B. V. B. Sarkissian, and B. R. Coles, J. Phys. F **10**, L333 (1980).

[12] In spite of several attempts by different groups, so far Y_9Co_7 was not obtained in a single-crystalline form.

[13] A. Kołodziejczyk and C. Sułkowski, J. Phys. F **15**, 1151 (1985).

[14] A. Kołodziejczyk, B. Wiendlocha, R. Zalecki, J. Toboła, and S. Kaprzyk, Acta Phys. Pol. A **111**, 513 (2007).

[15] B. Wiendlocha, J. Toboła, S. Kaprzyk, and A. Kołodziejczyk, Phys. Rev. B **83**, 094408 (2011).

[16] A. K. Grover, B. R. Coles, B. V. B. Sarkissian, and H. E. N. Stone, J. Less-Common Met. **86**, 29 (1982).

[17] K. Yvon, H. F. Braun, and E. Gratz, J. Phys. F **13**, L131 (1983).

[18] A. Kołodziejczyk, J. Leciejewicz, A. Szytuła, J. Chmist, and J. Węgrzyn, Acta Phys. Pol. A **72**, 319 (1987).

[19] The only exception are the $M(T)$ results shown in the main panel of Fig. 1. These data were collected after the resistivity measurements.

[20] B. V. B. Sarkissian, J. Phys. F **16**, 755 (1986).

[21] W. Cheng, G. Creuzet, P. Garoche, I. A. Campbell, and E. Gratz, J. Phys. F **12**, 475 (1982).

[22] C. H. Wu and Y. C. Chuang, J. Phase Equilib. **12**, 587 (1991).

[23] T. Klimczuk, V. A. Sidorov, A. Szajek, M. Werwiński, S. A. J. Kimber, A. L. Kozub, D. Safarik, J. D. Thompson, and R. J. Cava, J. Phys. Condens. Matter **25**, 125701 (2013).

[24] T. Moriya, *Fluctuations in Itinerant Electron Magnetism* (Springer, Berlin, 1985).

[25] D. Aoki and J. Flouquet, J. Phys. Soc. Jpn. **83**, 061011 (2014).

[26] K. Prokeš, A. de Visser, Y. K. Huang, B. Fåk, and E. Ressouche, Phys. Rev. B **81**, 180407 (2010).

[27] A. Steppke, R. Küchler, S. Lausberg, E. Lengyel, L. Steinke, R. Borth, T. Lühmann, C. Krellner, M. Nicklas, C. Geibel, F. Steglich, and M. Brando, Science **339**, 933 (2013).

[28] $T = 20$ K is the upper limit of our home-built high-resolution resistance setup.

[29] A. B. Pippard, *Magnetoresistance in Metals* (Cambridge University Press, Cambridge, 1989).

[30] S. B. Dugdale, H. M. Fretwell, M. A. Alam, G. Kontrym-Sznajd, R. N. West, and S. Badrzadeh, Phys. Rev. Lett. **79**, 941 (1997).

[31] G. J. McMullan, D. D. Pilgram, and A. Marshall, Phys. Rev. B **46**, 3789 (1992).

[32] K. Rogacki, A. Kołodziejczyk, Ł. Bochenek, and T. Cichorek, Philos. Mag. **95**, 503 (2015).

[33] A. Lewicki, Z. Tarnawski, C. Kapusta, A. Kołodziejczyk, H. Figiel, J. Chmist, Z. Lalowicz, and L. Śniadower, J. Magn. Magn. Mater. **36**, 297 (1983).

[34] R. G. Oraltay, J. J. M. Franse, P. E. Brommer, and A. Menovsky, J. Phys. F **14**, 737 (1984).

[35] C. Y. Huang, C. E. Olsen, W. W. Fuller, J. H. Huang, and S. A. Wolf, Solid State Commun. **45**, 795 (1983).